PHYSICAL REVIEW A **89**, 063415 (2014)

Synthetic Lorentz force in classical atomic gases via Doppler effect and radiation pressure

T. Dubček,[1] N. Šantić,[1] D. Jukić,[1,2] D. Aumiler,[3] T. Ban,[3] and H. Buljan[1,*]
[1]*Department of Physics, University of Zagreb, Bijenička cesta 32, HR-10000 Zagreb, Croatia*
[2]*Max Planck Institute for the Physics of Complex Systems, Nöthnitzer Straße 38, D-01187 Dresden, Germany*
[3]*Institute of Physics, Bijenička cesta 46, HR-10000 Zagreb, Croatia*
(Received 28 February 2014; published 18 June 2014)

We theoretically predict synthetic Lorentz force for classical (cold) atomic gases, which is based on the Doppler effect and radiation pressure. A fairly spatially uniform and strong force can be constructed for gases in macroscopic volumes of several cubic millimeters and more. This opens the possibility to mimic classical charged gases in magnetic fields in cold-atom experiments.

DOI: 10.1103/PhysRevA.89.063415 PACS number(s): 37.10.Vz

The quest for synthetic magnetism in quantum degenerate atomic gases is motivated by producing controllable quantum emulators, which could mimic complex quantum systems such as interacting electrons in magnetic fields [1]. An appealing idea is to place the atomic gas in a specially tailored laser field which, due to laser-atom interactions, acts as a synthetic magnetic field for neutral atoms [2]. The mechanism is based on the analogy between the Aharonov-Bohm phase accumulated when a charged quantum particle undergoes a closed loop in a magnetic field, and the Berry phase accumulated when an atom adiabatically traverses a closed loop in the tailored laser field [2,3].

Recent experiments in bulk Bose-Einstein condensates (BECs) have produced synthetic magnetic fields by spatially dependent optical coupling between the internal states of the atoms [4,5]. Superfluid vortices [4] and the Hall effect [5] were observed as signatures of synthetic magnetism in those BECs. Synthetic magnetism in optical lattices is achieved by engineering the complex tunneling parameter between the lattice sites, which is experimentally accomplished by different means [6,7]. Interestingly, even Dirac monopoles were observed in a synthetic magnetic field produced by a spinor BEC [8]. Synthetic magnetic fields for light (e.g., see Ref. [9]) are also attractive. Recently they were observed in deformed honeycomb photonic lattices [10]. Noninertial effects were studied in rotating waveguide arrays [11].

However, *classical* (rather than quantum degenerate) cold atomic gases have been circumvented in the quest for synthetic magnetism, even though they could emulate in a controllable fashion, and in tabletop experiments, versatile complex classical systems (e.g., see Refs. [12,13]); one desirable system for tabletop emulation is the tokamak plasma. We emphasize that here we consider classical atomic gases. This differs from using quantum degenerate gases to mimic frustrated classical magnetism in Ref. [12]. Laser forces on atoms in classical gases can generally depend on atomic velocity [14] and position [15]. A typical example is the Doppler cooling force—a viscous damping force that cools a classical gas to μK temperatures [14,15]. Here we demonstrate a scheme for creating a synthetic Lorentz force via the Doppler effect and radiation pressure, which is applicable for classical cold atomic gases. The experimental realization of the scheme is proposed with ^{87}Rb atoms cooled in a magneto-optical trap (MOT). The signature of the Lorentz force can be observed in the motion of the center of mass (CM) and/or the shape of the atomic cloud.

Numerous schemes have been proposed to create synthetic magnetic fields with ultracold atoms (see Refs. [1,2,16] for reviews). In the approach based on the Berry phase [3], when atoms move in space, they adiabatically follow the ground state of the light-atom coupling (dressed state), which depends on the spatial coordinates [2,3]. Their CM wave function acquires a geometric (Berry) phase, which corresponds to the gauge potentials [2]. The synthetic magnetic (and electric [17]) fields are derived from these gauge potentials [2]. In these schemes spontaneous emission must be minimized to prevent heating of the ultracold gas. For this reason, the dressed (ground) state is often a superposition of quasidegenerate ground states [3,18,19], i.e., the population of excited states is negligible [18,19]. A semiclassical interpretation of geometric gauge potentials, i.e., the connection with the Lorentz force, was reported in Ref. [20].

Another avenue for creating artificial magnetic fields in ultracold atomic gases is to rotate the system at some angular frequency, which provides the synthetic Lorentz force in the rotating frame [16]; the role of the Lorentz force is played by the Coriolis force. This scheme is suitable for rotationally invariant trapping potentials. However, the laser-atom interaction avenue is more appealing since it does not impose symmetries and produces synthetic magnetic fields in the laboratory frame [2].

In classical atomic gases, any scheme for synthetic magnetism must be operational on atoms moving with fairly large velocities (at least up to $\sim$0.5 m/s). The Berry phase method demanding adiabatic dynamics is therefore limited [2]. On the other hand, schemes for classical gases do not need to be limited by avoiding spontaneous emission. Next, classical gases in a standard MOT are typically of millimeter size [15] and the synthetic Lorentz force should therefore be large in volumes of at least a few cubic millimeters. With these guidelines in mind, it seems prosperous to seek for a scheme using laser-atom interactions for creating synthetic Lorentz forces, which would be specially designed for classical atomic gases.

The scheme proposed here is based on the Doppler effect and radiation pressure. The standard Doppler cooling force arises when a laser field is red detuned compared to the atomic resonance frequency as sketched in Fig. 1(a) [14,15].

*hbuljan@phy.hr

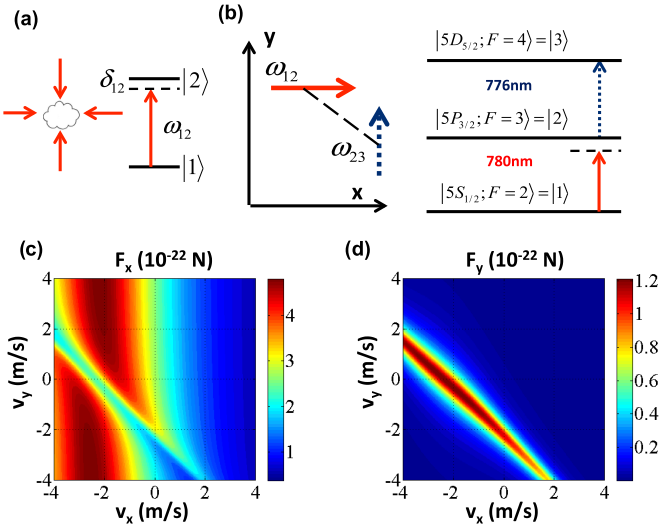

FIG. 1. (Color online) Sketch of the main idea for constructing the synthetic Lorentz force. (a) Illustration of the setup for the standard Doppler cooling force (using two-level atoms). (b) The idea for the synthetic Lorentz force in the simplest three-level system that can be realized with ^{87}Rb atoms. The dashed line indicates that two-step absorption of $\omega_{12}+\omega_{23}$ yields F_y. The force components (c) F_x and (d) F_y calculated as a function of the atomic velocity. See text for details.

Due to the Doppler effect, the atom has a greater probability for absorbing a photon when it moves towards the light source. Absorption changes the atom's momentum along the laser propagation axis, whereas spontaneously emitted photons yield random kicks. Cycles of absorption and emission result in a viscous damping force $\mathbf{F}_D(\mathbf{v}) \approx -\alpha\mathbf{v}$ for small velocities [15]; this force is collinear with the velocity and is used to obtain optical molasses [15].

Our first objective is to construct a laser-atom system (in the xy plane) where F_y depends on v_x. To achieve this via Doppler effect we utilize the multilevel structure of atoms. The simplest scheme is sketched in Fig. 1(b), where a three-level atom interacts with two orthogonal laser beams (linearly polarized along z). The laser ω_{12} is red detuned, $\delta_{12}=\omega_{12}-(E_2-E_1)\hbar^{-1}<0$, whereas ω_{23} is on resonance, $\delta_{23}=0$. The absorption of ω_{23} photons, which results in F_y, is the second step in the two-step, two-photon absorption process: $|1\rangle\rightarrow|2\rangle\rightarrow|3\rangle$. The probability for the two-step absorption depends on the Doppler-shifted detuning values $\delta_{12}-k_{12}v_x$ and $\delta_{23}-k_{23}v_y$, which provides the desired dependence of F_y on v_x. The maximum in F_y is expected for atoms with velocity $(v_x=\delta_{12}/k_{12}, v_y=\delta_{23}/k_{23})$, i.e., when each of the two steps is resonant.

The force can be calculated by using density matrices and the Ehrenfest theorem as described in detail in Ref. [15]. First we (numerically) solve the optical Bloch equations to find the stationary density matrix $\hat{\rho}$ for an atom with velocity $\mathbf{v}$; the matrix elements are $\rho_{ij}=\sigma_{ij}e^{i\omega_{ij}t}=\rho^*_{ji}$, and $d\sigma_{ij}/dt=0$; ω_{ij} is the frequency of the laser driving the transition $|i\rangle\rightarrow|j\rangle$. In the calculation, the following parameters are used [15]: the energies E_j of the levels participating in the interaction $(j=1,\ldots,N)$, the Rabi frequencies Ω_{ij}, detuning values δ_{ij}, the wave vectors $\mathbf{k}_{ij}$ of the lasers, and the decay parameters of the excited states (Γ_{ji} is the decay rate via $|j\rangle\rightarrow|i\rangle$; the total width of state $|j\rangle$ is $\Gamma_j=\sum_{i<j}\Gamma_{ji}$). The force is given by $\mathbf{F}=\langle-\nabla_r\hat{H}\rangle=-\mathrm{Tr}(\hat{\rho}\nabla_r\hat{H})$, where $\hat{H}$ is the Hamiltonian associated with the dipole interaction, and $\nabla_r=\hat{\mathbf{x}}\partial/\partial x+\hat{\mathbf{y}}\partial/\partial y$ [15]. For plane (traveling) waves used here, $\mathbf{F}=-\sum_{i=1}^{N-1}\sum_{j=i+1}^{N}\hbar\mathbf{k}_{ij}\,\mathrm{Im}(\sigma_{ij}\Omega^*_{ij})$. The density matrix depends on the Doppler-shifted detuning values $\delta_{ij}-\mathbf{k}_{ij}\cdot\mathbf{v}$, which provides the velocity dependence of the force [15].

It should be emphasized that the ideas for constructing synthetic Lorentz forces presented here are general and potentially applicable to various atomic species. For concreteness, the ideas are presented for ^{87}Rb atoms using experimentally relevant atomic states and transitions. The three-level system that can be used to experimentally realize the simplest scheme is presented in Fig. 1(b). The transition wavelengths are $\lambda_{12}=780$ nm [21] and $\lambda_{23}=776$ nm [22]. The decay rate of the $|5P_{3/2}\rangle$ hyperfine states is $\Gamma_P=2\pi\times6.1$ MHz [21], and $\Gamma_D=2\pi\times0.66$ MHz for $|5D_{5/2}\rangle$ states [22]; the decay pattern is $\Gamma_{32}=\Gamma_D$, $\Gamma_{31}=0$, and $\Gamma_{21}=\Gamma_P$ [21,22]. In Figs. 1(c) and 1(d) we illustrate $\mathbf{F}(\mathbf{v})$ for detuning values $\delta_{12}=-0.5\Gamma_P$, $\delta_{23}=0$, and Rabi frequencies $\Omega_{12}=0.12\Gamma_P$, and $\Omega_{13}=0.34\Gamma_P$. As expected, the maximum of the force F_y occurs when $v_x=\delta_{12}/k_{12}$ and $v_y=\delta_{23}/k_{23}$. Interestingly, $F_y(v_x,v_y)$ has the shape of a mountain ridge peaked at $\delta_{12}+\delta_{23}-k_{12}v_x-k_{23}v_y=0$. This is a consequence of the fact that the intermediate state $|2\rangle$ is much broader than state $|3\rangle$. For the two-step absorption to be effective, the Doppler-shifted detuning of the first photon should roughly be $|\delta_{12}-k_{12}v_x|<\Gamma_2$, and the total detuning $|\delta_{12}+\delta_{23}-k_{12}v_x-k_{23}v_y|<\Gamma_3$; since $\Gamma_3\ll\Gamma_2$, the velocities satisfying these inequalities are close to the ridge line. The ridge can be shifted in the v_xv_y plane by changing the detuning values. The scheme above illustrates the main idea towards constructing the synthetic Lorentz force via the Doppler effect.

Note that the force in the x direction is also altered for atoms with velocities at the ridge. The presence of the second-step transition $|2\rangle\rightarrow|3\rangle$ changes the populations of all three levels, which affects the rate of the first-step transition $|1\rangle\rightarrow|2\rangle$ and hence F_x. It should be noted that deformations of the ridge can arise for larger Rabi frequencies due to the Autler-Townes effect [23].

In order to provide a general framework for our scheme we Taylor expand the force in velocity up to the linear term:

$$\begin{bmatrix}F_x\\F_y\end{bmatrix}=\begin{bmatrix}F_{x0}\\F_{y0}\end{bmatrix}+\begin{bmatrix}\alpha_{xx}&0\\0&\alpha_{yy}\end{bmatrix}\begin{bmatrix}v_x\\v_y\end{bmatrix}+\begin{bmatrix}0&\alpha_{xy}\\\alpha_{yx}&0\end{bmatrix}\begin{bmatrix}v_x\\v_y\end{bmatrix}$$

$$=\mathbf{F}_0+\mathbf{F}_D(\mathbf{v})+\mathbf{F}_{\mathrm{SL}}(\mathbf{v}). \quad (1)$$

Here $\alpha_{ij}=\partial F_i/\partial v_j$ evaluated at $\mathbf{v}=0$ $(i,j\in\{x,y\})$. This form is often an excellent approximation for $\mathbf{F}(\mathbf{v})$ because of the small velocities of cold atoms. The third term $\mathbf{F}_{\mathrm{SL}}(\mathbf{v})$ is a general form of the synthetic Lorentz force with components perpendicular to the velocity components: $F_{\mathrm{SL},x}=\alpha_{xy}v_y$, $F_{\mathrm{SL},y}=\alpha_{yx}v_x$ [24]. The force on a standing atom is $\mathbf{F}_0$; the components of the standard Doppler force are $F_{D,x}=\alpha_{xx}v_x$, and $F_{D,y}=\alpha_{yy}v_y$. When $\alpha_{xy}=-\alpha_{yx}$, $\mathbf{F}_{\mathrm{SL}}$ takes the form of the standard Lorentz force, $\mathbf{F}_{\mathrm{SL}}=\mathbf{v}\times\mathbf{B}^*$, where $\mathbf{B}^*=\alpha_{xy}\hat{\mathbf{z}}$ [24].

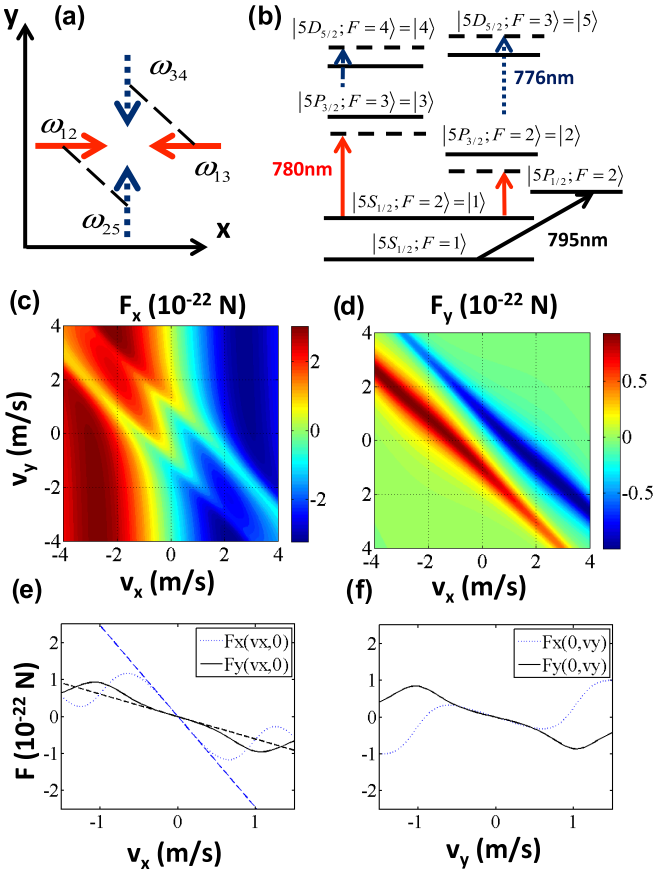

FIG. 2. (Color online) The five-level scheme. (a) The symmetric configuration of lasers for creating the synthetic Lorentz force, and (b) its realization with hyperfine ^{87}Rb levels. Density plots of (c) F_x and (d) F_y as a function of velocity. Cross sections (e) $F_x(v_x,0)$ and $F_y(v_x,0)$ and (f) $F_x(0,v_y)$ and $F_y(0,v_y)$. See text for details.

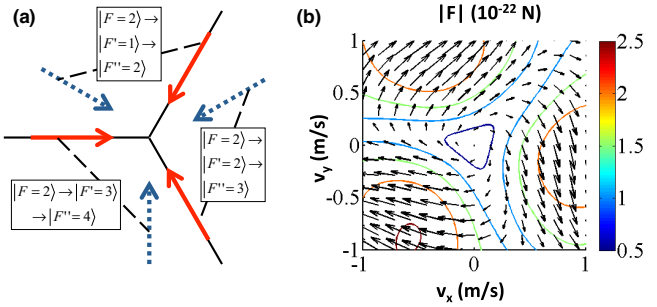

FIG. 3. (Color online) The tripod configuration of the three two-step excitations arms, and the obtained force. (a) Red solid arrows depict first-step excitations (red detuned), and blue dotted arrows depict second steps (blue detuned). Black dashed lines connect beams that correspond to one arm; $|F=2\rangle$ denotes the $5S_{1/2}$ hyperfine state, $|F'=1,2,3\rangle$ denote three $5P_{3/2}$ hyperfine states, and $|F''=2,3,4\rangle$ denote three $5D_{5/2}$ hyperfine states. (b) Contour lines and length of the arrows correspond to the magnitude of the force $|\mathbf{F}(\mathbf{v})|$.

Let us illustrate a few force patterns $\mathbf{F}(\mathbf{v})$ that can be achieved with our scheme. Consider a system of five-level atoms and two orthogonal pairs of counterpropagating beams depicted in Fig. 2(a). This is simply a generalization of the idea presented in Fig. 1 with a symmetric pair of two-step arms such that $\mathbf{F}_0 = \mathbf{0}$. It can be experimentally realized by using hyperfine levels of ^{87}Rb depicted in Fig. 2(b); the use of a repumper laser is mandatory since the chosen five-level system is not closed: $|5P_{3/2};F=2\rangle \xrightarrow{50\%} |5S_{1/2};F=1\rangle = |0\rangle \xrightarrow{795\text{ nm}} |5P_{1/2};F=2\rangle = |6\rangle \xrightarrow{50\%} |5S_{1/2};F=2\rangle$ (this is included in our calculations). The Rabi frequencies and detuning values for the transitions are $\Omega_{12}=\Omega_{13}=0.11\Gamma_P$, and $\delta_{12}=\delta_{13}=-0.5\Gamma_P$. The pairs of beams along x are red detuned, while the pairs along y are blue detuned (by a smaller magnitude): $\delta_{25}=\delta_{34}=0.25\Gamma_P$; $\Omega_{25}=\Omega_{34}=0.38\Gamma_P$. The repumper is on resonance with high intensity $\Omega_{06}=1.77\Gamma_P$, in a standing-wave configuration (it does not produce net force on atoms). The decay pattern is given by $\Gamma_{21}=\Gamma_{20}=0.5\Gamma_P$, $\Gamma_{31}=\Gamma_P$, $\Gamma_{43}=\Gamma_D$, $\Gamma_{53}=0.2\Gamma_D$, $\Gamma_{52}=0.8\Gamma_D$, and $\Gamma_{60}=\Gamma_{61}=0.5\Gamma_P$; the rest of $\Gamma_{ji}=0$. In Figs. 2(c) and 2(d) we show the force $\mathbf{F}(\mathbf{v})$. Atoms moving towards the left (right) will experience $F_y>0$ ($F_y<0$, respectively). From Figs. 2(e) and 2(f) we see that the force depends linearly on the velocity v_x for velocities below $\sim$0.7 m/s (which includes essentially all atoms in a standard ^{87}Rb MOT [15]). The two ridges in F_y correspond to the pair of arms of the two-step absorption; their position and shape was explained in Fig. 1(d). By changing the detuning values, the ridges can be shifted in the v_xv_y plane, which changes the parameters α_{ij} and therefore the strength of the synthetic Lorentz force.

It should be noted that because our approach is based on the Doppler effect, it usually also yields the Doppler (cooling) force $\mathbf{F}_D$. If for some reason this is not wanted, dissipation can be diminished (for example, by using one blue-detuned and one red-detuned laser in the counterpropagating configuration for the first-step excitation). Moreover, the synthetic force can be made of the form $\mathbf{v}\times\mathbf{B}^*$: By using three arms of the two-step scheme at 120° [Fig. 3(a)], one can obtain the force plotted in Fig. 3(b). Two arms are identical as in Fig. 2(b), and the third arm is $|5S_{1/2};F=2\rangle \to |5P_{3/2};F=1\rangle \to |5D_{5/2};F=2\rangle$. The Rabi frequency of the first (second) step in all arms is $0.11\Gamma_P$ ($0.77\Gamma_P$); the detuning values are $-0.5\Gamma_P$ ($0.25\Gamma_P$) for the first (second) step. Clearly, the force rotates around zero in the v_xv_y plane. Strictly, the force field is invariant under rotation by 120°, however, for small velocities it is effectively rotationally invariant. By fitting $\mathbf{F}(\mathbf{v})$ to Eq. (1) we obtain $\alpha_{xy}=-\alpha_{yx}=0.23\times10^{-21}$ N s/m, i.e., $\mathbf{B}^*=\alpha_{xy}\hat{\mathbf{z}}$. The cyclotron frequency for ^{87}Rb atoms corresponding to our forces is $\alpha_{xy}/m\approx1.6$ kHz. It should be emphasized that, because we are using hyperfine levels of ^{87}Rb, the scheme can be achieved with two cw lasers at 780 and 776 nm by using acoustic optical modulators (AOMs), i.e., it is experimentally viable.

The prediction of the synthetic Lorentz force is made for individual atoms, however, we should propose its signature in the CM motion and/or shape of a cold atomic cloud containing a huge number (say, $\sim10^9$ [15]) of atoms. To this end we propose a quench-type scenario(s). First, we assume that an atomic cloud is present in the MOT, and cooled to mK–μK temperatures. The laser fields driving the MOT have much larger Rabi frequencies than lasers producing a synthetic Lorentz force. The latter will slightly heat up the cloud, but will not change its shape. Then, at $t=0$, the MOT lasers

and the magnetic field are suddenly turned off (it can be done within less than 1 μs, which is essentially instantaneous for this system). After $t = 0$, the cloud starts moving in the presence of the synthetic Lorentz and Doppler forces. We focus on dynamics in the xy plane. Moreover, we assume that gravity is in the z direction and does not influence observations. The typical experimental observation time for the measurements proposed here is 5–10 ms; an initially standing atom will fall for 0.12–0.49 mm. The laser fields creating the synthetic Lorentz forces can be made of a much larger diameter (on the order of several cm). Since the dynamics in the xy plane is independent of the dynamics in the z plane, we do not expect a significant influence of gravity on our predictions below.

We will discuss two scenarios for the force plotted in Fig. 2. First, if the cloud is given an initial velocity ($v_x = 0.15$ m/s, $v_y = 0$), it will move along x due to inertia, but its CM will also move in the negative y direction due to the synthetic Lorentz force. After 10 ms the shift in y is $\sim$0.2 mm, which is observable in MOT experiments. The initial velocity can be achieved by inducing oscillations of the cloud in the MOT trap for $t < 0$ (e.g., see Ref. [25]).

Second, we discuss expansion of the cloud by employing the Fokker-Planck equation [15]

$$\frac{\partial P(\mathbf{x},\mathbf{v},t)}{\partial t} + \mathbf{v}\cdot\nabla_r P = \frac{-1}{m}\nabla_v\cdot[(\mathbf{F}_D + \mathbf{F}_{\rm SL})P] + \frac{D}{m^2}\nabla_v^2 P. \tag{2}$$

Here, $P(\mathbf{x},\mathbf{v},t)$ is the distribution of particles in the phase space; D is the diffusion constant, approximately given by $D \approx (\hbar k)^2 \sum_j \rho_{jj}\Gamma_j$ [15], where $k \approx 2\pi/780$ nm^{-1}; $\nabla_v = \hat{\mathbf{x}}\partial/\partial v_x + \hat{\mathbf{y}}\partial/\partial v_y$. For forces $\mathbf{F}_D + \mathbf{F}_{\rm SL}$ linearized in velocity (1), the Fokker-Planck equation is solved by the ansatz

$$P(x,y,v_x,v_y,t) = P_0 \exp\left\{-\sum_{ij=1}^{4}\frac{1}{2}a_{ij}(t)\eta_i\eta_j\right\}, \tag{3}$$

where $(\eta_1,\eta_2,\eta_3,\eta_4) = (x,y,v_x,v_y)$; after inserting (3) in Eq. (2), one obtains ten coupled ordinary differential equations (ODEs) for the functions $a_{ij}(t)$, ten because $a_{ij} = a_{ji}$ by construction. These coupled ODEs are solved numerically and the results are plotted in Fig. 4 for the following parameters: $(\alpha_{xx},\alpha_{xy},\alpha_{yx},\alpha_{yy}) = -(2.4,0.60,0.69,0.58)\times10^{-22}$ N s/m, and $D/m_{\rm Rb}^2 = 31$ m^2 s^{-3}; the initial state is $P = P_0$ $\exp\{-(\mathbf{x}/x_0)^2-(\mathbf{v}/v_0)^2\}$, where x_0=1 mm, and v_0=0.25 m/s.

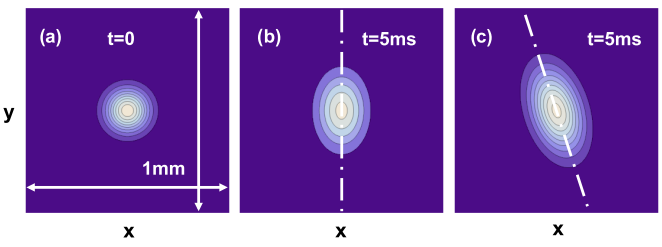

FIG. 4. (Color online) Dynamics of the shape of the cloud during expansion in the presence of a synthetic Lorentz force $\mathbf{F}_{\rm SL}(\mathbf{v})$ and/or Doppler force $\mathbf{F}_D(\mathbf{v})$. The force corresponds to that from Fig. 2. (a) Density of the cloud at $t = 0$, (b) after 5 ms of expansion under the action of $\mathbf{F}_D(\mathbf{v})$, and (c) after 5 ms expansion in the presence of $\mathbf{F}_D(\mathbf{v}) + \mathbf{F}_{\rm SL}(\mathbf{v})$. See text for details.

Starting from a centrosymmetric cloud plotted in Fig. 4(a), in the presence of solely the Doppler force, the cloud expands asymmetrically [Fig. 4(b)] because $|\alpha_{xx}| > |\alpha_{yy}|$. The signature of the synthetic Lorentz force is the rotation of the asymmetric cloud in the xy plane during expansion [see Fig. 4(c)]. The interpretation is simple: Particles moving to the left (right) are pushed up (down), as can be inferred from Fig. 2(d). There is another effect: The change in F_y for a given atomic velocity group also changes F_x for that group, as discussed above. For the parameters corresponding to Figs. 2 and 4, besides the targeted $\alpha_{yx} < 0$, we incidentally also obtained $\alpha_{xy} < 0$ (for small velocities) which also contributes to rotation. Note that expansion in the rotationally symmetric force field presented in Fig. 3 would cause the rotation of atoms around the center, but this would not be visible in the density (in the proposed scenario it is essential to have $|\alpha_{xx}| \neq |\alpha_{yy}|$). By shining a red-detuned laser beam in the plane of such a rotationally invariant but rotating cloud, one would have different absorption in the part of the cloud moving towards (away) from the laser beam due to the Doppler effect; this seems to be one viable scheme to observe rotation of the cloud.

Before closing, let us discuss specific approximations that we used here to simplify the calculation. First, we neglected the absorption of the lasers in the cold atomic cloud. Absorption changes the intensity of beams across the cloud, and therefore introduces spatial dependence of the synthetic Lorentz force (and not only the velocity dependence). This effect can be reduced by using clouds with a lower density (say, 10^9 atoms per cm^3), or by using lasers with a higher intensity (closer to saturation). The latter approach will also increase the diffusion coefficient. Second, in our proposal we neglected the Zeeman structure of the atomic levels. This simplification is acceptable when the dynamics of the cloud does not occur in a magnetic field (i.e., Zeeman splitting is absent), as in the two scenarios described above. Next, the dipole moments of different transitions used in the scheme will be generally different (they also depend on the polarization of the light used). The key goal one has to achieve is to have the same Rabi frequencies for all first (second) steps in each arm, as in our examples above. In experiments, this can be realized by using light of different intensities in steps that have different transition dipole moments. This could in principle be achieved by balancing the forces arising from different arms. Finally, let us note that the internal dynamics occurs on a much faster time scale than CM motion; the bottleneck for internal dynamics is the lifetime of the $5D_{5/2}$ state of 240 ns, whereas the typical time scale for CM motion is 1 ms.

In conclusion, we have demonstrated a scheme for creating synthetic Lorentz forces in cold classical atomic clouds, based on the Doppler effect and radiation pressure. We envision that following these ideas, one could design cold-gas experiments to mimic classical charged gases in magnetic fields. One desired classical system for emulation is the tokamak plasma. A necessary (but not sufficient) step towards this goal is to have a scheme for producing synthetic magnetic fields for classical gases. The next step towards mimicking the tokamak plasma would be to construct a toroidal synthetic magnetic field, which is beyond the scope of this paper. Here we have predicted synthetic Lorentz forces of magnitude $F/v \approx 0.23\times10^{-21}$ N s/m in macroscopic volumes of a few mm^3 and more. The maximal

volume depends on the intensities of lasers; with standard diode lasers one could achieve the synthetic Lorentz force in at least 1 cm^3. As a reference point we note that the obtained force on a unit charge particle (of any mass) is produced by a magnetic field of 1.5 mT. The cyclotron frequency (which includes the particle mass) for ^{87}Rb atoms corresponding to our forces is $F/(mv) \approx 1.6$ kHz, which is large enough to see the phenomena associated with the synthetic Lorentz force on the time scale of the envisioned experiments. Even stronger forces can be achieved for larger intensities of the lasers at the expense of more heating and diffusion. We envision that our concept involving two-photon absorption could be applicable in other systems, e.g., for suspended nanoparticles with a nonlinear index of refraction where one laser beam would induce an index change, and thus influence the force of another (say, perpendicular) beam on the particle. The concept holds the potential to be used for velocity selection in atomic beams.

This work was supported by the Unity through Knowledge Fund (UKF Grant No. 5/13). We are grateful to A. Eckardt, J. Radić, Th. Gasenzer, and A. Vardi for a critical reading of the manuscript.

[1] I. Bloch, J. Dalibard, and S. Nascimbene, Nat. Phys. **8**, 267 (2012).
[2] J. Dalibard, F. Gerbier, G. Juzeliunas, and P. Öhberg, Rev. Mod. Phys. **83**, 1523 (2011).
[3] R. Dum and M. Olshanii, Phys. Rev. Lett. **76**, 1788 (1996).
[4] Y-J. Lin, R. L. Compton, K. Jiménez-García, J. V. Porto, and I. B. Spielman, Nature (London) **462**, 628 (2009).
[5] L. J. Le Blanc, K. Jiménez-García, R. A. Williams, M. C. Beeler, A. R. Perry, W. D. Phillips, and I. B. Spielman, Proc. Natl. Acad. Sci. USA **109**, 10811 (2012).
[6] M. Aidelsburger, M. Atala, S. Nascimbene, S. Trotzky, Y.-A. Chen, and I. Bloch, Phys. Rev. Lett. **107**, 255301 (2011).
[7] J. Struck, C. Ölschläger, M. Weinberg, P. Hauke, J. Simonet, A. Eckardt, M. Lewenstein, K. Sengstock, and P. Windpassinger, Phys. Rev. Lett. **108**, 225304 (2012).
[8] M. W. Ray, E. Ruokokoski, S. Kandel, M. Mottonen, and D. S. Hall, Nature (London) **505**, 657 (2014).
[9] I. Carusotto and C. Ciuti, Rev. Mod. Phys. **85**, 299 (2013).
[10] M. C. Rechtsman, J. M. Zeuner, A. Tünnermann, S. Nolte, M. Segev, and A. Szameit, Nat. Photon. **7**, 153 (2012).
[11] S. Jia and J. W. Fleischer, Phys. Rev. A **79**, 041804(R) (2009).
[12] J. Struck, Ölschläger, R. Le Targat, P. Soltan-Panahi, A. Eckardt, M. Lewenstein, P. Windpassinger, and K. Sengstock, Science **333**, 996 (2011).
[13] Q. Baudouin, W. Guerin, and R. Kaiser, in *Annual Review of Cold Atoms and Molecules*, edited by K. Madison, Y. Wang, A. M. Rey, and K. Bongs (World Scientific, Singapore, 2014), Vol. 2.
[14] S. Chu, L. Hollberg, J. E. Bjorkholm, A. Cable, and A. Ashkin, Phys. Rev. Lett. **55**, 48 (1985).
[15] H. J. Metcalf and P. Van Der Straten, *Laser Cooling and Trapping* (Springer, New York, 1999).
[16] N. R. Cooper, Adv. Phys. **57**, 539 (2008).
[17] Y. J. Lin, R. L. Compton, K. Jiménez-García, W. D. Phillips, J. V. Porto, and I. B. Spielman, Nat. Phys. **7**, 531 (2011).
[18] G. Juzeliunas and P. Öhberg, Phys. Rev. Lett. **93**, 033602 (2004).
[19] G. Juzeliunas, J. Ruseckas, P. Öhberg, and M. Fleischhauer, Phys. Rev. A **73**, 025602 (2006).
[20] M. Cheneau, S. P. Rath, T. Yefsah, K. J. Günter, G. Juzeliunas, and J. Dalibard, Europhys. Lett. **83**, 60001 (2008).
[21] D. A. Steck, http://steck.us/alkalidata/rubidium87numbers.pdf
[22] D. Sheng, A. Perez Galvan, and L. A. Orozco, Phys. Rev. A **78**, 062506 (2008).
[23] S. H. Autler and C. H. Townes, Phys. Rev. **100**, 703 (1955).
[24] The definition of the synthetic Lorentz force in Eq. (1) is broader than the form $\mathbf{v}\times\mathbf{B}^*$, but includes that standard form.
[25] X. Xu, Th. H. Loftus, M. J. Smith, J. L. Hall, A. Gallagher, and J. Ye, Phys. Rev. A **66**, 011401(R) (2002).